

Local Pre-Conditioning and Quality Enhancement to Handle Different Data Complexities in Contactless Fingerprint Classification

Deepika K C¹

Dept. of Electronics and Communication
Malnad College of Engineering
Hassan, Karnataka, India

G Shivakumar²

Dept. of Electronics and Instrumentation
Malnad College of Engineering
Hassan, Karnataka, India

Abstract—Biometric authentication systems have always been a fascinating approach to meet personalized security. Among the major existing solutions fingerprint-biometrics have gained widespread attention; yet, guaranteeing scalability and reliability over real-time demands remains a challenge. Despite innovations, the recent COVID-19 pandemic has capped the efficacy of the existing touch-based two-dimensional fingerprint detection models. Though, touchless fingerprint detection is considered as a viable alternative; yet, the real-time data complexities like non-linear textural patterns, dusts, non-uniform local conditions like illumination, contrast, orientation make it complex for realization. Moreover, the likelihood of ridge discontinuity and spatio-temporal texture damages can limit its efficacy. Considering these complexities, here, we focused on improving the input image intrinsic feature characteristics. More specifically, applied normalization, ridge orientation estimation, ridge frequency estimation, ridge masking and Gabor filtering over the input touchless fingerprint images. The proposed model mainly focusses on reducing FPR & EER by dividing the input image in to blocks and classify each input block as recoverable and nonrecoverable image block. Finally, an image with higher recoverable blocks with sufficiently large intrinsic features were considered for feature extraction and classification. The Proposed method outperforms when compared with the existing state of the art methods by achieving an accuracy of 94.72%, precision of 98.84%, recall of 97.716%, F-Measure 0.9827, specificity of 95.38% and a reduced EER of about 0.084.

Keywords—Ridge orientation; Gabor filtering; region masking; ridge frequency; contactless fingerprint

I. INTRODUCTION

The last few decades have witnessed exponential rise in advanced technologies, including software computing, decentralized computing, smart intelligence, sensor and hardware systems. Despite significant innovation and technological horizon, personalized security or system security often remains a challenge under dynamic application environment [1]. Whether it is data, channel or infrastructure, guaranteeing security for these key systems has remained as an open challenge for academia-industries [2]. In the last few years, the rise in attack events too has increased significantly. The different attacks models have been developed on the basis of the exploiting user's or system access credentials like passwords, smart card attack loss, impersonation, Brute Force attacks etc. [1][2]. Most of these attacks have resulted huge

data losses and breach, financial losses, system failure, and even the loss of life. Unlike cryptographic concepts, in the last few years biometric driven authentication systems have increased significantly [4][5] having superior potential with high scalability, interoperability and time-efficiency. Its efficacy can easily be visualized as Aadhar Card system by Unique Identification Authority of India (UIAI) [17]. Interestingly, more than a billion of population in India possesses a fingerprint driven Aadhar card for its verification. Though, Aadhar is a multi-modal system; however, evolved with fingerprint identification. In contemporary world whether it is corporate official attendance systems, entry or exit or even attendance systems in schools, fingerprint had remained a viable choice. In sync with such significances, a large number of efforts have been made by academia-industries; however, the recent pandemic of COVID-19 has limited the scope of the classical touch-based fingerprint authentication systems [6]. COVID-19 pandemic has almost limited the efficacy of the touch-based two-dimensional fingerprint driven modalities, as this pandemic was found exponentially spreading due to inter-personal infection through such frequently touching devices [14][15]. For instance, in certain offices, an executive could be seen trying his/her fingers many times to get system access. Fun, apart, but the severity of such frequent problems is high in real-world applications. The local conditions like sensor efficiency, optimality, sample distortion, scratches and humidity etc. often impact efficacy of the classical touch-based fingerprint techniques [3][7]. To alleviate such issues, improving feature modality in conjunction with contactless identification system seems to be the motivation for academia-industry for future efforts [8-12]. Noticeably, unlike touch-based two-dimensional feature learning environment, retrieving fingerprint feature under different orientation, lighting conditions is a complex problem. Moreover, suffer from the low accuracy and hence such system often undergoes false positive under varied local feature conditions and spatio-temporal complexities. Therefore, to cope up with touchless fingerprint identification system demands, researchers require improving local conditions, feature modalities as well as learning environment [13][16]. These key scopes are considered as the key driving forces behind this study.

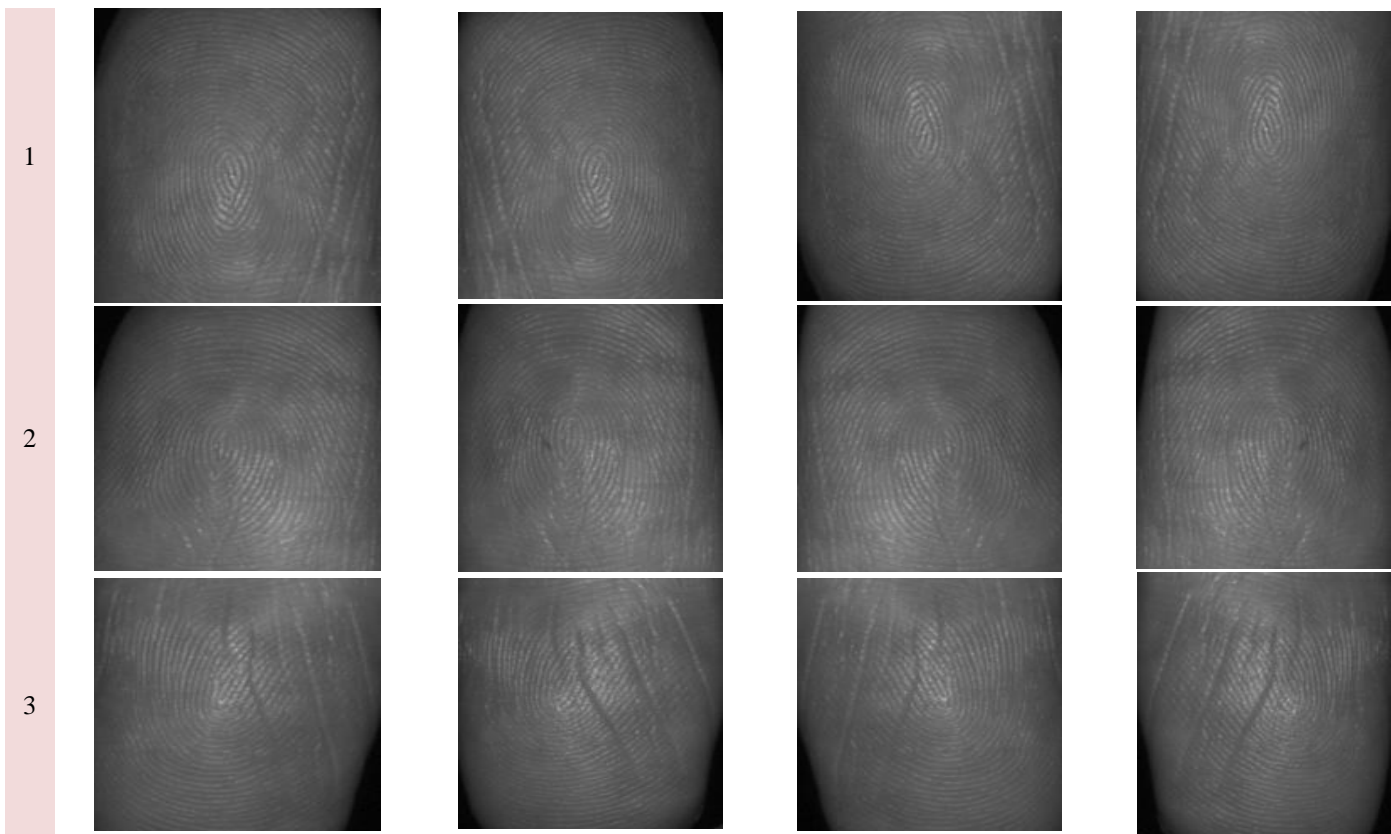
In the last few years very few but significant efforts have been made towards touchless fingerprint detection methods. Jonietz et al. [3] recently tried to use depth camera and mobile

devices to perform touchless fingerprint detection. Despite RGB image and depth information combination, the key problem of non-uniform cues over feature space makes it limited towards realistic purposes. To alleviate such issues, Pang et al. [18] derived a three-dimensional feature model from input image that helped in improving ridge-valley information. To achieve it, authors at first employed least square method to fit a local paraboloid surface that helped estimating the local surface curvature and tensors curvature. Though, this approach helped in improving ridge-value orientation and depth information; however, at the cost of increased computation. Unlike previous works, Jonietz et al. [19] designed touchless finger detection model exploited aggregated channel features with RGB color space for finger segmentation that in conjunction with geometric shape helped estimating the fingertip for verification. Zaghetto et al. [20] too made effort to alleviate issues primarily caused due to orientational complexity and resulting spatio-temporal feature changes. To achieve it, authors applied Multiview scanner with multilayer neuro-computing. Despite their ability to address bad positioning problem, they could achieve the highest accuracy of 94%, which still needed to be improved. Though, Galbally et al. [8] made effort to improve accuracy by applying Laser sensing technique named 3D: FLARE. Yet, this approach was limited to yield a scalable solution for real-world purposes. Noticeably, these all approaches failed in providing a solution with scalability and efficacy towards real-world

application. However, the depth assessment indicates that improving local input condition with superior feature segmentation and learning can yield superior performance.

Considering above stated key issues and allied scopes in this research, the emphasis was made on multi-dimensional optimization including pre-processing, feature extraction and eventual learning model. Being touchless approach, we considered normal three-dimensional RGB images as input, which is then processed for histogram equalization followed by contrast improvement and filtering. Recalling, non-linear ridge value patterns and local textural variations, we performed image normalization using Z-score method. Here, we performed block-wise normalization to improve contrast information. Subsequently, orientation image estimation was performed to improve local feature distribution. Moreover, it enabled frequency image estimation to make further spatio-temporal feature learning better. As post frequency image estimation, we performed ridge mask generation and Gabor filtering to ensure optimal local spatio-temporal feature (STTF) distribution for further minutiae detection. Unlike classical approaches, we performed three-dimensional minutiae projection and ridge mapping that improved overall feature space to achieve better spatio-temporal features for further learning. Finally, cropping the improved ridge mapping information, we performed deep-STTF feature extraction by applying Gray-level Co-occurrence Matrix (GLCM) followed by classification using random forest algorithm.

TABLE I. ILLUSTRATION OF 3D CONTACTLESS FINGERPRINT SAMPLES



II. METHODOLOGY

This section focuses on improving input data environment to ensure reliable fingerprint detection. In major touchless fingerprint detection models the viewing angle, image orientation, loss of ridges or damaged ridges and furrow structure, varying lighting or contrast etc. often impacts features, that eventually influences overall prediction accuracy. Considering this fact, in this paper, we focused on alleviating local data complexities. Moreover, we intend to guarantee intrinsic feature driven local conditioning so as to make optimal feature extraction without depending on the classical minutiae detection and segmentation. To achieve it, the proposed work encompasses data acquisition, Local Pre-conditioning and Image Quality Enhancement followed by feature extraction, classification and performance analysis.

A. Data Acquisition

In sync with the targeted contactless environment for fingerprint detection system, in this work we collected contactless three-dimensional sensor driven images to prepare datasets. The 3D touchless fingerprint datasets were collected in such a manner that it could enable effective learning under data heterogeneity and diversity to make it more efficient under realistic environment. Training over the large heterogeneous fingerprint patterns can make artificial intelligence driven models robust towards realistic purposes. Moreover, it can help achieving high reliability. We considered the 3D Fingerprint dataset comprising a large contactless fingerprint sample. Noticeably, for our case study we considered a total of 50 subjects and the samples collected were from the subjects aged in between 28 to 55 years. The subjects comprised a total of 40 man and 10 women that eventually contributed 160 and 40 fingerprint samples, correspondingly. The data considered had been collected under natural light conditions with standard illumination. Here, no specific light or illumination control measure was applied. To introduce diversity in reference to the viewing angle, illumination, contrast, orientation etc., subjects were instructed to stand in-front of the camera; and were instructed to move freely while keeping target fingers within camera vision range. Though, the similar dataset named 3D-FLRE-DB retrieves each fingerprint sample 15 times, where five different samples were obtained at a specific speed; we considered data retrieval at the random movement without any pre-calibrated speed definition. To introduce mode STTF feature heterogeneity the samples were not collected consecutively rather were captured at the different interval or gaps. To achieve it, once capturing one sample from a subject, the sample from another subject was captured, and this process was followed across the sample collection process over target subject volume. This approach was primarily done to introduce high spatial variability and textural heterogeneity to improve learning efficiency. A snippet of the data considered in this study is given in Table I.

1) *Preliminary*: Let, I be the input fingerprint image with $N \times N$ dimensional matrix, with $I(i, j)$ as the pixel intensity for the i th row and the j th column. In sync with touchless input, we hypothesize that the input images possess minimum resolution of 600 dots per inch, which is not difficult in contemporary high-definition camera. Thus, for the input

images with aforesaid specification, the mean and the variance of the fingerprint image I in its gray-level form are derived as equation (1) and (2) respectively.

$$M(I) = \frac{1}{N^2} \sum_{i=0}^{N-1} \sum_{j=0}^{N-1} I(i, j) \quad (1)$$

$$Var(I) = \frac{1}{N^2} \sum_{i=0}^{N-1} \sum_{j=0}^{N-1} (I(i, j) - M(I))^2 \quad (2)$$

B. Local Pre-conditioning and Image Quality Enhancement

The overall proposed local pre-conditioning model encompasses the following key processes:

- Image Normalization.
- Local Orientation Estimation.
- Local Frequency Estimation.
- Ridge Masking.
- Gabor Filtering and Smoothing.

The proposed model at first performed normalization in such a manner that it retains a pre-defined mean and variance characterized.

2) *Image normalization*: Consider $I(i, j)$ be the gray-level value for the input touchless fingerprint image where (i, j) be the corresponding pixel values. Moreover, let M and Var be the measured mean and variance of the input image I . In this case, the normalized gray-level image for the input $I(i, j)$ can be obtained as $G(i, j)$, which is mathematically derived as per equation (3).

$$G(i, j) = \begin{cases} M_0 + \sqrt{\frac{Var_0(I(i, j) - M)^2}{Var}}, & \text{if } I(i, j) > M \\ M_0 - \sqrt{\frac{Var_0(I(i, j) - M)^2}{Var}}, & \text{Otherwise} \end{cases} \quad (3)$$

In (3), M_0 and Var_0 represents the expected mean and the variance values, correspondingly. In the proposed model, normalization is performed as a pixel-wise function and therefore it retained the native image clarity, especially ridge-and-furrow structure for further feature extraction and learning. Here, the key motive was to minimize the variations in the gray-level values in the direction of ridges and furrows so as to enable further processes more efficient without losing any intrinsic information.

3) *Ridge orientation estimation*: In reference to the touchless fingerprint, where the input image can have spatio-temporal differences caused because of varying light conditions, change in orientation, spatial and temporal feature non-linearity. To ensure optimal feature learning, we focused on improving ridge STTF. To achieve improved ridge information and allied intrinsic values, we performed ridge orientation estimation. In this work, we designed a least-mean square image orientation estimation concept for orientation image estimation. The proposed Ridge Orientation Image Estimation model is accomplished in multiple sequential steps. A snippet of the involved algorithm and allied implementation is given as follows:

Step-1: Split the input Gray-level image in $w \times w$ dimension. Here, we considered 64×64 dimension to split input image into multiple grids.

Step-2: Estimate the gradient information in x and y directions for each pixel element (i, j) . Here, the gradient in x and y directions were, $\delta_x(i, j)$ and $\delta_y(i, j)$, respectively for the input pixel elements (i, j) . In this work, to ensure low computational overheads over a large input image, we applied Sobel operator method to perform gradient estimation.

Step-3: Measure the local orientation values for each input block, especially centered at the pixel element (i, j) by applying following mathematical formula.

$$V_x(i, j) = \sum_{u=i-\frac{w}{2}}^{i+\frac{w}{2}} \sum_{v=j-\frac{w}{2}}^{j+\frac{w}{2}} 2\delta_x(u, v)\delta_y(u, v) \quad (4)$$

$$V_y(i, j) = \sum_{u=i-\frac{w}{2}}^{i+\frac{w}{2}} \sum_{v=j-\frac{w}{2}}^{j+\frac{w}{2}} (\delta_x^2(u, v) - \delta_y^2(u, v)) \quad (5)$$

$$\theta(i, j) = \frac{1}{2} \tan^{-1} \left(\frac{V_y(i, j)}{V_x(i, j)} \right) \quad (6)$$

In (6), $\theta(i, j)$ represents the LMS value of the local ridge orientation for the block centred at the pixel location (i, j) . In fact, ridge orientation signifies the direction which is orthogonal to the dominant direction of the Fourier spectrum over $w \times w$ window.

Step-4: This is the matter of fact that unlike touch-based fingerprint detection models, touchless image driven approaches might undergo more noise, reflections, dust related problems. In addition, touchless images can have the likelihood of the more damaged or corrupted ridge values or orientation, which can also be given rise due to the change in orientation or light intensity, contrast etc. Non-uniform skin surfaces too can show different spatio-temporal distribution for the ridge and furrow values in touchless fingerprint images. In sync with such complexities and allied challenges, the estimated values of the local ridge orientation can become inaccurate as well at certain time. In reference to these issues, we recall a hypothesis stating that as the local ridge orientation values vary gradually in local vicinity, especially in those neighboring localities where there is no singular point takes place or appear. In this reference, the use of a low-pass filter can be employed to manipulate the incorrect local ridge estimation (6). Now, to achieve it the orientation image is converted into a continuous vector field (CVF), which is mathematically derived as per (7) and (8). In above (7) and (8), the variables Φ_x and Φ_y represent the x and y components of the vector fields, correspondingly.

$$\Phi_x(x, y) = \cos(2\theta(i, j)) \quad (7)$$

$$\Phi_y(x, y) = \sin(2\theta(i, j)) \quad (8)$$

Then performed LPF filtering by applying following mathematical approaches (9-10).

$$\Phi'_x(i, j) = \sum_{u=-\frac{w_\Phi}{2}}^{\frac{w_\Phi}{2}} \sum_{v=-\frac{w_\Phi}{2}}^{\frac{w_\Phi}{2}} W(u, v)\Phi_x(i - uw, j - vw) \quad (9)$$

$$\Phi'_y(i, j) = \sum_{u=-\frac{w_\Phi}{2}}^{\frac{w_\Phi}{2}} \sum_{v=-\frac{w_\Phi}{2}}^{\frac{w_\Phi}{2}} W(u, v)\Phi_y(i - uw, j - vw) \quad (10)$$

In (9-10), the parameter W represents the two-dimensional LPF possessing single integral where the size of the filter is considered as $w_\Phi \times w_\Phi$. We performed smoothing at the block level where the filter size was fixed as 5×5 .

Step-5: Update the local ridge orientation at the pixel position (i, j) by using (11).

$$O(i, j) = \frac{1}{2} \tan \left(\frac{\Phi'_y(i, j)}{\Phi'_x(i, j)} \right) \quad (11)$$

Thus, applying above stated approach of smoothening and allied orientation image estimation we obtained a uniformly oriented field image, which is consequently processed for frequency estimation.

4) *Ridge frequency estimation*: As stated in the previous sections, in case of touchless fingerprint images, especially when there are no minutiae in certain neighborhood, the gray-level values along ridges can be reconstructed as a sinusoidal wave. Noticeably, these sinusoidal-shaped waves are modelled towards the direction orthogonal to the local ridge orientation. Because of this reason, another key intrinsic feature from the input fingerprint images can be obtained in the form of local ridge frequency estimation. In other words, similar to the ridge orientation, ridge frequency can be modelled as an intrinsic feature for the touchless fingerprint images. In the proposed model, to estimate the ridge frequency information in a neighborhood we employed the pre-estimated measures like normalized image and the ridge orientation images. Let, G and O be the normalized and the orientation images, respectively. Then, with these values, we estimated ridge frequency using following sequential implementation approach.

Step-1: Split the input Gray-level image in 64×64 dimension.

Step-2: Estimate the orientation window with fixed size $l \times w$ (128×64) over each block, centred at the pixel information (i, j) .

Step-3: In reference to the Step-2, estimate the x -signature ($X[0], X[1], \dots, X[l-1]$) of the ridges within the window, conditioned at:

$$X[k] = \frac{1}{w} \sum_{d=0}^{w-1} G(u, v), k = 0, 1, \dots, l-1 \quad (12)$$

$$u = i + \left(d - \frac{w}{2} \right) \cos O(i, j) + \left(k - \frac{l}{2} \right) \sin O(i, j) \quad (13)$$

$$u = j + \left(d - \frac{w}{2} \right) \sin O(i, j) + \left(\frac{l}{2} - k \right) \cos O(i, j) \quad (14)$$

In case there exists no minutiae in the oriented window, the x -signature constitutes a discrete sinusoidal-shape wave, possessing the similar frequency as that of the ridges in oriented window. This as a result, enables estimation of the ridge frequency from x -signature. Consider that $T(i, j)$ be the mean pixel counts in between the two subsequent peaks in the x -signature, then the ridge frequency $\Omega(i, j)$ is measured as per (15).

$$\Omega(i, j) = \frac{1}{T(i, j)} \quad (15)$$

In case there is no consecutive peaks available in x-signature, then the frequency is assigned a fixed value -1 that helps in differentiating it from the genuine frequency values.

Step-4: In case, the fingerprint images are taken over a predefined and definite resolution, then the value of frequency of the ridges within certain vicinity remains within a definite range. In case of 600 dots per inch resolution (DPI) this range remains within the level of $\left[\frac{1}{3}, \frac{1}{25}\right]$. In this manner, in case the measured value of the frequency becomes higher than the above stated range, the frequency is assigned a value -1, signifying that no genuine frequency could be estimated or observed.

Step-5: In touchless fingerprint images and corresponding blocks where the minutiae or ridges are corrupted due to any local or personal regions, it doesn't constitute any well-structured sinusoidal wave. In this case, it becomes inevitable to interpolate those frequency values of those specific blocks from the frequency of the adjacent blocks possessing well-structured frequency. Here, we applied the following measures to perform interpolation, over each block centered at the pixel location (i, j) .

$$\Omega'(i, j) = \begin{cases} \Omega(i, j) & \text{if } \Omega(i, j) \neq -1 \\ \frac{\sum_{u=w_{\Omega/2}}^{w_{\Omega/2}} \sum_{l=w_{\Omega/2}}^{w_{\Omega/2}} W_g(u, v) \mu(\Omega(i-uw, j-uw))}{\sum_{u=w_{\Omega/2}}^{w_{\Omega/2}} \sum_{l=w_{\Omega/2}}^{w_{\Omega/2}} W_g(u, v) \delta(\Omega(i-uw, j-uw)+1)} & \text{Otherwise} \end{cases} \quad (16)$$

$$\text{Where, } \mu(x) = \begin{cases} 0, & \text{if } x \leq 0 \\ x, & \text{Otherwise} \end{cases}$$

$$\delta(x) = \begin{cases} 0, & \text{if } x \leq 0 \\ 1, & \text{Otherwise} \end{cases} \quad (17)$$

In (16), W_g refers the discrete Gaussian kernel with mean and variance are assigned as 0 and 9, correspondingly. Here, the other components w_{Ω} be the size of kernels which was fixed at 7. In case there exists minimum one block possessing the frequency value of -1, then the value of Ω is swapped to Ω' , and the above stated process is repeated (Step-5).

Step-6: Considering the gradual change in the inter-ridge distance variation, the proposed model applies LPF to eliminate the outliers.

$$F(i, j) = \sum_{u=w_{\Omega/2}}^{w_{\Omega/2}} \sum_{l=w_{\Omega/2}}^{w_{\Omega/2}} W_t(u, v) \Omega'(i-uw, j-uw) \quad (18)$$

In (18), W_t represents the two-dimensional LPF with single integral, while $W_t = 7$ be the filter's size.

5) *Ridge masking*: As stated above, in real-time touchless fingerprint image a block or allied pixel can be either in non-recoverable or recoverable region. And therefore, classification of the blocks or pixels in above stated categories can be done on the basis of the wave's shape analysis. In this work, we employed three distinct features including amplitude (α), frequency (β) and variance (γ). Consider that, $X[1], X[2], \dots, X[l]$ be the x-signature of a specific block

centered at the pixel position (i, j) , then the aforesaid three different features pertaining to that block are obtained as per the following approach.

Step-1: Assign the value of α as the mean height of the peak and the mean depth of the valley.

Step-2: Define β as $\frac{1}{T(i, j)}$, where $T(i, j)$ refers the number of pixels in between the two consecutive peaks (average value).

Step-3: Estimate the value of variance γ , as per (19).

$$\gamma = \frac{1}{l} \sum_{i=1}^l \left(X[i] - \left(\frac{1}{l} \sum_{i=1}^l X[i] \right) \right)^2 \quad (19)$$

Thus, applying this method we estimated a large number of three-dimensional patterns for each input image. Moreover, k-NN classifier was applied to classify each block of $w \times w$ dimension that classifies each input block as recoverable or non-recoverable so as to help identifying the most suitable set of feature blocks for feature extraction. In case a block was found recoverable, the corresponding region was estimated. In case, the fraction of the recoverable region was lower in comparison to a predefined threshold ($T_{Threshold} = 40$), we dropped that image for further feature extraction and learning. Finally, an image with higher recoverable image with sufficiently large intrinsic features were considered for further feature extraction and learning, so as to improve fingerprint detection and classification. Here, we label the recoverable region $R(i, j)$ as 1, while non-recoverable region is labelled as 0. Now, once identifying the optimal set of intrinsically enriched images, we performed filtering to improve spatio-temporal feature distribution. The details of the filtering method applied is given in the subsequent section.

6) *Gabor filtering and smoothing*: This is the matter of fact that the structure of the parallel ridges in fingerprint image, especially possessing well-structured orientation and frequency can provide sufficiently large intrinsic information to drop irrelevant and noisy components. On the other hand, the sinusoid waves pertaining to the ridges too change gradually in the local fixed orientation. Because of this reason, a bandpass filter can be designed in such a manner that it would eliminate all unexpected or undesired noise components, while retaining the true ridge information for further learning. In reference to this scope, Gabor filter can be a viable solution as it possesses both orientation-selective characteristics as well as frequency-selective characteristics in both frequency as well as spatial domains. Considering this fact, we applied Gabor filter as the bandpass filter to eliminate noise components while preserving genuine ridge structures in fingerprint images. The Gabor filter can typically be presented as (20).

$$h(x, y: \phi, f) = \exp \left\{ \frac{1}{2} \left[\frac{(xcos\phi)^2}{\delta_x^2} + \frac{(ysin\phi)^2}{\delta_y^2} \right] \right\} \cos(2\pi f cos\phi) \quad (20)$$

where ϕ refers the Gabor filter's orientation, while f represents the frequency of a sinusoidal wave. The components

δ_x and δ_y be the space constants pertaining to the Gaussian envelope towards x and y , correspondingly. Here, the modulation transfer function of the considered filter is stated as per (21).

$$H(u, v; \phi, f) = 2\pi\delta_x\delta_y \exp\left\{-\frac{1}{2}\left[\frac{[(u-2\pi/f)\sin\phi]^2}{\delta_u^2} + \frac{(u\cos\phi)^2}{\delta_v^2}\right]\right\} + 2\pi\delta_x\delta_y \exp\left\{-\frac{1}{2}\left[\frac{[(u-2\pi/f)\sin\phi]^2}{\delta_u^2} + \frac{(u\cos\phi)^2}{\delta_v^2}\right]\right\} \quad (21)$$

In (21), $\delta_u = 1/2\pi\delta_x$ and $\delta_v = 1/2\pi\delta_y$.

To implement Gabor filters over each input touchless fingerprint image, three different parameters including the frequency of the sinusoidal wave u_0 , filter orientation and standard deviation of the Gaussian envelope in the different directions δ_x and δ_y , are considered. Here, the frequency characteristics of the filter f is estimated by employing local ridge frequency and the ridge orientation values. In the proposed model, the selection of trade-off between δ_x and δ_y is maintained in such a manner that higher the trade-off, more noise tolerant. However, it might cause spurious ridge information. On the contrary, smaller the values, the lower the Gaussian envelope, δ_x and δ_y . However, it might be less effective towards noise elimination. In this work, δ_x and δ_y values were assigned as 4.0, each. Now, consider that the input gray-level input fingerprint image be G , O be the ridge orientation image, while F be the ridge frequency image, and R be the recoverable mask. Then, the improved fingerprint image ε is obtained using the following equation.

$$\varepsilon(i, j) = \begin{cases} 255, & \text{if } R(i, j) = 0 \\ \sum_{u=-w_g/2}^{w_g/2} \sum_{v=-w_g/2}^{w_g/2} h(u, v; O(i, j), F(i, j))G(i-u, j-v), & \text{Otherwise} \end{cases} \quad (22)$$

Thus, the final local pre-conditioned and improved fingerprint images are processed further for the feature extraction and identification.

C. GLCM Driven STTF Textural Features Extraction and Classification

In this research work, GLCM functions as a descriptive statistical feature distribution model assessing the probability of the pixel's gray scale values over an input fingerprint image. Functionally, it extracts high-dimensional statistical features. In this work, the varied STTF features are distributed uniformly throughout the pre-processed input image. In this work, over each input fingerprint image we extracted the different STTF features, which were later combined together to yield a composite feature vector for learning and classification. In this method, the retrieved spatio-temporal textural features were derived in the form of a matrix representing pixel intensities $I(x, y)$, centered on the pixels (x, y) . In this manner, we extracted different spatio-temporal textural features for each input pre-processed images, with distinct probability matrix $P_{i,j}$. Here, the above stated probability matrix signifies the differences of the intensity between the pixel elements i and j that later helps in detecting motion patterns. In GLCM gray-scale refers the pair association along a direction, and therefore retrieving the gray-scale values can yield a matrix representing the association matrix among the pixels towards the target

direction. We obtained symmetric matrix S by amalgamating the gray-scale information along with the allied transpose values. It enables estimation of the cumulative relationship among pixels in one direction. We normalized the symmetric association matrix S using (23) to obtain the probability matrix $P_{i,j}$.

$$P_{i,j} = \frac{S_{i,j}}{\sum_{i,j=0}^{N-1} S_{i,j}} \quad (23)$$

With the extracted values of $P_{i,j}$, the different STTF features including Contrast, Energy, Homogeneity, Correlation, Mean, Standard deviation, Variance, Kurtosis and Skewness are obtained. As stated, a total of nine STTF features were obtained for further feature learning. Here, our predominant goal was to retain maximum possible and significant features for learning and classification so as to achieve higher accuracy.

Once extracting above stated nine different GLCM features, we performed horizontal concatenation to estimate a composite feature vector for further learning. The composite GLCM feature obtained is given in equation (24).

$$GLCM_{Feat} = Conc \begin{pmatrix} CONT, ENE, HOM, CORR, \\ Mean, Var, STD, Kur, Skw \end{pmatrix} \quad (24)$$

Now, once estimating the composite feature vector ($GLCM_{Feat}$), we projected it for feature learning and classification. As stated, in this work we intended to exploit maximum possible feature instances to ensure optimal learning by Random Forest learning method and hence classification accuracy.

III. RESULTS AND DISCUSSION

As stated above, in this section we mainly focus on assessing efficacy of the proposed contactless fingerprint detection and classification model, qualitatively as well as quantitatively. In other words, here we examine whether the use of local pre-conditioned image improvement yields superior performance. Before discussing the simulation results quantitatively, a snippet of pre-conditioned and enhanced results is given as follows.

Fig. 1(a) presents a random input 3D touchless fingerprint image. Here, it can easily be visualized that the illumination at the image center and bottom is relatively higher in comparison to the top corners. Moreover, the ridge structures in lower right bottom are unclear with high level of ambiguity. Furthermore, the straight division lines on the left side (bottom to top) can easily be visualized in this sample image, which can disrupt the ridge continuity to make further feature segmentation or allied feature learning. Noticeably, there are numerous local conditions such as low temperature, salty water contact by which the ridge values get changed temporarily. Though, with touch-based classical methods while pressing finger over the sensor, such local deformations get suppressed; however, in touchless fingerprint detection it can have decisive impact on feature learning and hence classification. To alleviate such issues, we performed local pre-conditioning to improve the ridge quality for further feature extraction. As repeatedly stated in the previous sections, we intended to guarantee ridge continuity over the different local conditions while ensuring that the ridges contain sufficient intrinsic features. To achieve

it, we applied the different pre-processing steps like image normalization, ridge orientation estimation, frequency estimation, ridge masking and filtering. Fig. 1(b) presents the normalized image output obtained from the original input image. Here, the impact of normalization can easily be visualized. Now, recalling the methodological intend where we intended to improve ridge structure continuity even over non-linear textural fingerprint surfaces, we performed ridge orientation estimation as shown in Fig. 1(c). The ridge frequency obtained over each grid is given in Fig. 1(d). In Fig. 1(e) presents the ridge masking results where the high frequent ridges are masked as 1, while the less frequent ridges are labelled as 0. Here, the key motive was to retain the ridge information carrying densely distributed features. The improved ridge structure is obtained by filtering (Fig. 1(f)). Here, observing the results it can easily be understood that the improved 3D touchless fingerprint image carries more uniform ridge's distribution with precisely perceptible structure, which can provide more efficient feature vectors for further learning and classification. The other images (Fig. 1(g) and Fig. 1(h)) represent the binary images, where 1(g) depicts the binarized image over the input (1(f)). Observing the bottom of the binarized image (Fig. 1(g)), it can be found that the bottom of the image carries ambiguities primarily because of ridge and furrow diversity, conjunction and non-linear bifurcation, random cuts etc. This as a result can impact STTF textural features and hence overall fingerprint detection accuracy. However, retaining a threshold driven approach can retain only feature intensive components to perform further feature and classification. Thus, observing the results in Fig. 1, it can be stated that the inclusion of the proposed model can yield superior feature vector for further learning and classification. Noticeably, in our proposed model to perform feature

extraction we considered the improved ridge image (Fig. 1(f)) as input, which is hypothesized to yield superior performance.

The statistical performance outputs were measured by obtaining confusion matrix in terms of Accuracy, Precision, F-measure, Specificity, Recall and EER and are listed in Table II.

This is the matter of fact that a large number of studies have been done towards touch-based fingerprint detection systems; however, the efforts made towards touchless fingerprint detection are countable and very rare. Our depth literature assessment revealed that merely countable a dozen of efforts is made so far to introduce 3D touchless data for fingerprint detection. To assess relative performance, we have selected the recent methods like [8-12]. Ritesh and Ajay [9] developed a collaborative paradigm by exploiting ridge-valley minutiae information to perform contactless fingerprint detection. In their effort, authors mainly focused on improving minutiae under complex input data environment (like unclear ridge bifurcation, varied viewing angle and allied textural gradience). Moreover, authors tried to suppress spurious minutiae information so as to improve accuracy and reliability.

TABLE II. PERFORMANCE ASSESSMENT

	Proposed method
Accuracy	94.72%
Precision	98.84%
Recall	97.71%
Specificity	95.38%
F-measure	0.9827
Equal Error Rate	0.084

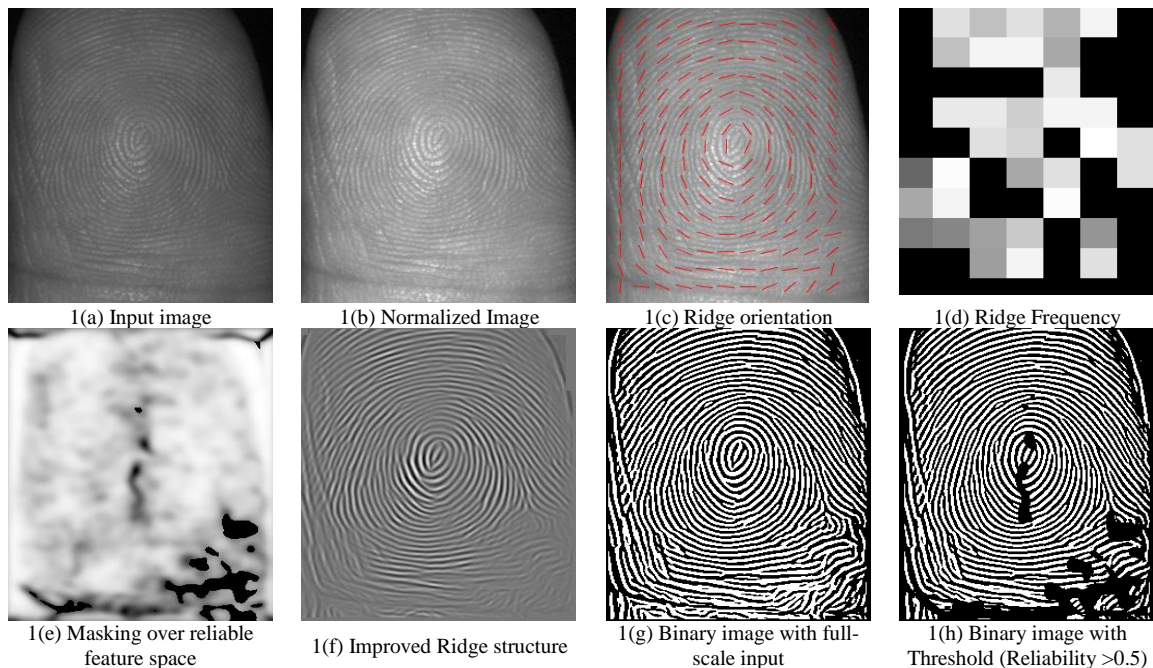


Fig. 1. Pre-conditioned and Enhanced Results by the Proposed Method.

Authors applied the different datasets or fingerprint matchers like NBIS Biometric Image Software, MCC, and COTS (Commercial off-the-shelf), and therefore obtained the different performance over the different benchmark data. Interestingly, over the NBIS matcher they could achieve the EER of 13.33%. Noticeably, in comparison to their effort our proposed model exhibited EER of 0.084%. It shows superiority of our proposed model over the existing approach [9]. Recently, Galbally et al. [8] developed 3D-FLARE, a touchless fingerprint detection model; however. Despite the fact that their approach was quite complex in real-world realization, it exhibited EER of 10.03%. Though, to alleviate aforesaid data environment complexities, authors [8] made effort to segment yaw angle with fingerprint and fingertip separation etc., which was followed by hybrid feature extraction using local binary patterns (LBP) and Histograms of Oriented Gradient (HOG) features. Authors applied LBP+HOG features obtained from the segmented features to perform classification.

Authors could achieve the average EER of 10.03%, which is still higher than our proposed model. Kumar and Kwong [10] proposed a single camera driven touchless fingerprint detection model. In fact, it was a 3D minutia matching concept that made effort to recover extended 3D fingerprint features from the reconstructed 3D fingerprints. The EER performance

by authors [10] was 1.02%, which is far more than our proposed model. An improved model by Lin and Kumar [11] applied deep learning driven multi-view touchless fingerprint detection model. This approach exploited multi-view deep representation to perform touchless fingerprint detection. Their proposed model [11] encompassed convolutional neural network where one fully convolutional network was applied to perform fingerprint segmentation, while three other layers were employed to learn 3D multi-view fingerprint feature representation. Undeniably, authors made effort to address at hand complexities with contactless fingerprint detection models that resulted into reduced EER value (0.64%). Zheng and Kumar [12] performed 3D fingerprint identification by exploiting recovered surface normal and albedo information. The key novelty of this approach was that it didn't require any surface reconstruction rather it employed different mathematical approaches to retrieve surface normal and albedo information, which was later used for learning and classification. The EER performed by this approach was 2.49%, which was higher than our proposed model. Thus, observing overall performance outcomes and allied inferences as shown in Fig. 2, it can be stated that the proposed touchless fingerprint detection model outperforms other state-of-the-art methods.

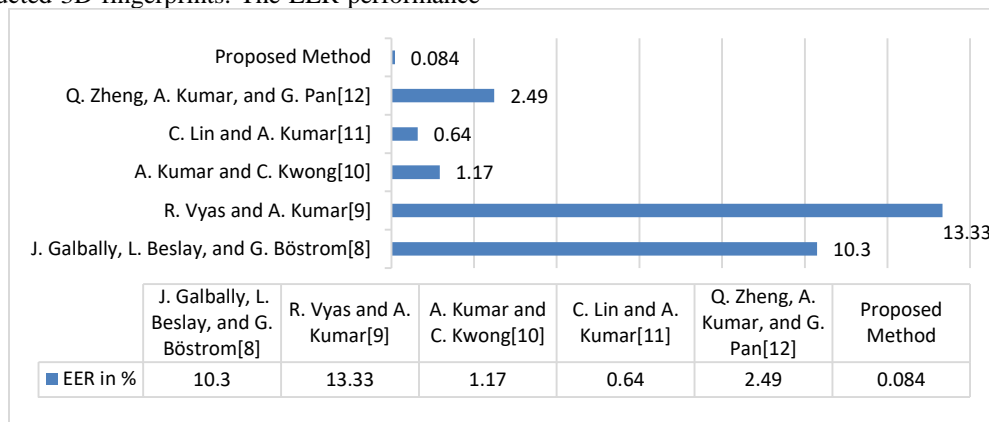


Fig. 2. Comparison of Equal Error rate of the Proposed Method with the Existing State-of-the-Art Methods.

IV. CONCLUSION

Since the inception, the fingerprint detection models have always been considered as a vital alternative of the classical cryptosystems. Undeniably, being fast in execution and diverse in spatio-temporal presentation, fingerprint-based systems turn out to be more efficient solution for personalized security and access control purposes. This efficacy makes fingerprint-based authentication system as one of the most used approaches for corporates, financial sectors, smart home and industrial monitoring and control. Despite robustness, being touch-based paradigm, its optimality has been challenges under different operating environment, especially in reference to the health and hygiene. During the recent pandemic of COVID-19, touch-based fingerprint models were found vulnerable due to touch-based infection probability. To alleviate such issues, contactless fingerprint detection method can be a viable solution; however, being touchless in nature such approaches might undergo different complexities like the impact of viewing angle, textural non-linearity, non-uniform illumination

and contrast, ridge and furrow ambiguity, ridge discontinuity, etc. On the other hand, extracting structural features or other STTF features over aforesaid local adversaries can impact overall efficacy. In other words, training over a feature obtained from ambiguous or minimally distinct spatio-temporal feature space can give rise to the high false positive rate (FPR) and Equal Error Rate (EER). To alleviate such problems, it requires multiple optimization measures including local quality improvement or ridge improvement, and information-rich feature extraction. To achieve it, at first a local pre-conditioning concept was derived that mainly focused on improving ridge's orientation and spatial presentation so that the optimal features could be extracted. Recalling the fact that extracting features over the ambiguous ridges or furrows or even over detached ridges can lead false positive, the proposed pre-processing model helped in alleviating aforesaid complexities. This approach eventually retains only those feature-rich spatial components having clearly observable or distinctly distributed ridges for reliable feature extraction and

classification. As a future work we can experiment with the different feature extraction methods and learning algorithms to improve the accuracy of classification. Efforts can also be made in feature extraction stage like using Deep Neural Networks to reduce the Equal Error Rate and False Positive rate.

ACKNOWLEDGMENT

The Authors would like to thank the management, Principal and authorities of Malnad College of Engineering, Hassan for extending full support in carrying out this research work.

REFERENCES

- [1] V. A. Thakor, M. A. Razaque and M. R. A. Khandaker, "Lightweight Cryptography Algorithms for Resource-Constrained IoT Devices: A Review, Comparison and Research Opportunities," in *IEEE Access*, vol. 9, pp. 28177-28193, 2021, doi: 10.1109/ACCESS.2021.3052867.
- [2] Krishna, P. G., & Muthuluru, N. Feistel network assisted dynamic keying based SPN lightweight encryption for IoT security. *International Journal of Advanced Computer Science and Applications*, 12(6). doi.org/10.14569/IJACSA.2021.0120642.
- [3] C. Jonietz and I. Jivet, "Touchless Fingerprint Capturing from RGB-D Images in Mobile Devices," 2018 International Symposium on Electronics and Telecommunications (ISETC), 2018, pp. 1-4, doi: 10.1109/ISETC.2018.8583879.
- [4] S. Ding, W. Bian, H. Liao, T. Sun and Y. Xue, "Combining Gabor filtering and classification dictionaries learning for fingerprint enhancement," in *IET Biometrics*, vol. 6, no. 6, pp. 438-447, 11 2017. https://doi.org/10.1049/iet-bmt.2016.0161.
- [5] X. Si, J. Feng, J. Zhou and Y. Luo, "Detection and Rectification of Distorted Fingerprints," in *IEEE Transactions on Pattern Analysis and Machine Intelligence*, vol. 37, no. 3, pp. 555-568, 1 March 2015, doi: 10.1109/TPAMI.2014.2345403.
- [6] N. Shanthy V, Aalelai Vendhan M. Rejuvenation of online research interactive fora during COVID-19. *Indian Journal of Science and Technology* .2020;13(47):4603605. https://doi.org/10.17485/IJST/v13i47.2230.
- [7] Deepika, K.C., Shivakumar, G. A, "Robust Deep Features Enabled Touchless 3D-Fingerprint Classification System". *SN Computer Science* , volume 2, Article number: 263 (2021). https://doi.org/10.1007/s42979-021-00657-x.
- [8] J. Galbally, L. Beslay and G. Böstrom, "3D-FLARE: A Touchless Full-3D Fingerprint Recognition System Based on Laser Sensing," in *IEEE Access*, vol. 8, pp. 145513-145534, 2020, doi: 10.1109/ACCESS.2020.3014796.
- [9] R. Vyas and A. Kumar, "A Collaborative Approach using Ridge-Valley Minutiae for More Accurate Contactless Fingerprint Identification", Technical Report No.: COMP-K-25, 2018, pp. 1-15. https://doi.org/10.48550/arXiv.1909.06045.
- [10] A. Kumar and C. Kwong, "Towards Contactless, Low-Cost and Accurate 3D Fingerprint Identification", *IEEE Transactions on Pattern Analysis and Machine Intelligence*, Vol. 37, No. 3, March 2015, pp. 681-696. https://doi.org/10.1109/CVPR.2013.441.
- [11] C. Lin and A. Kumar, "Contactless and Partial 3D Fingerprint Recognition using multi-view Deep Representation", *Pattern Recognition* (2018), DOI: 10.1016/j.patcog.2018.05.004.
- [12] Q. Zheng, A. Kumar and G. Pan, "Contactless 3D fingerprint identification without 3D reconstruction," 2018 International Workshop on Biometrics and Forensics (IWBF), 2018, pp. 1-6, doi: 10.1109/IWBF.2018.8401566.
- [13] K. C. Deepika and G. Shivakumar, "Hybrid CNN-Ensemble based Classifier for Touchless Fingerprint Classification," 2021 IEEE Mysore Sub Section International Conference (MysuruCon), 2021, pp. 482-486, https://doi:10.1109/MysuruCon52639.2021.9641718.
- [14] Q. D. Vo and P. De, "A Survey of Fingerprint-Based Outdoor Localization," in *IEEE Communications Surveys & Tutorials*, vol. 18, no. 1, pp. 491-506, Firstquarter 2016, doi: 10.1109/COMST.2015.2448632.
- [15] R. Kumar, P. Chandra and M. Hanmandlu, "Fingerprint Matching Using Rotational Invariant Image Based Descriptor and Machine Learning Techniques," 2013 6th International Conference on Emerging Trends in Engineering and Technology, 2013, pp. 13-18, doi: 10.1109/ICETET.2013.4.
- [16] Deepika K.C., Shivakumar G. (2021) Towards More Accurate Touchless Fingerprint Classification Using Deep Learning and SVM. *International Conference on Information Processing, Data Science and Computational Intelligence* pp 248–257, 2021. https://doi.org/10.1007/978-3-030-91244-4_20.
- [17] https://uidai.gov.in/.
- [18] X. Pang, Z. Song and W. Xie, "Extracting Valley-Ridge Lines from Point-Cloud-Based 3D Fingerprint Models," in *IEEE Computer Graphics and Applications*, vol. 33, no. 4, pp. 73-81, July-Aug. 2013, doi: 10.1109/MCG.2012.128.
- [19] C. Jonietz, E. Monari, H. Widak and C. Qu, "Towards mobile and touchless fingerprint verification," 2015 12th IEEE International Conference on Advanced Video and Signal Based Surveillance (AVSS), 2015, pp. 1-6, doi: 10.1109/AVSS.2015.7301751.
- [20] C. Zaghetto, B. Vidal and L. H. M. Aguiar, "Touchless multiview fingerprint quality assessment: rotational bad-positioning detection using Artificial Neural Networks," 2015 International Conference on Biometrics, 2015, pp. 394-399, doi: 10.1109/ICB.2015.713910.